NACA TN No. 1726

NATIONAL ADVISORY COMMITTEE FOR AERONAUTICS

TECHNICAL NOTE

No. 1726

SPRAY CHARACTERISTICS OF FOUR FLYING-BOAT HULLS AS AFFECTED BY LENGTH-BEAM RATIO

By William W. Hodges and David R. Woodward

Langley Aeronautical Laboratory
Langley Field, Va.

Washington
October 1948

NATIONAL ADVISORY COMMITTEE FOR AERONAUTICS

TECHNICAL NOTE NO. 1726

SPRAY CHARACTERISTICS OF FOUR FLYING-BOAT HULLS AS AFFECTED BY LENGTH-BEAM RATIO

By William W. Hodges and David R. Woodward

SUMMARY

An investigation of the spray characteristics in smooth water of four related models having length-beam ratios of 6, 9, 12, and 15 and constant values of length^2-beam product has been made in Langley tank no. 1. The parent model for the series was similar to a Navy twin-engine flying boat.

When forebody length^2-beam product was held constant, similar propeller and flap spray characteristics were obtained for hulls over a very wide range of length-beam ratio; however, higher length-beam ratios may require greater clearance between elevators and water.

The spray characteristics of the models agreed well with the spray criterion presented in NACA ARR No. 3K08. This criterion may be considered conservative for hulls with high length-beam ratios as shown by the fact that the models having length-beam ratios of 9, 12, and 15 operated at greater loads with no propeller spray than did the model having the conventional length-beam ratio of 6.

INTRODUCTION

The selection of over-all proportions of flying-boat hulls to ensure minimum air drag and adequate hydrodynamic performance is a difficult problem. Obviously the minimization of air drag is most readily accomplished by the reduction of hull frontal area and volume. Previous analyses (references 1 and 2) have indicated that increasing the length-beam ratio while hull length^2-beam product is held constant results in reducing the hull frontal area and volume and, at the same time, in maintaining similar hydrodynamic characteristics.

In order to afford designers an aid in selecting the hull proportions for high-speed and long-range flying boats, the National Advisory Committee for Aeronautics has developed a series of hulls ranging in length-beam ratio from 6 (the conventional ratio) to 15. The background for the derivation of the series is set forth in reference 1

where hulls of different length–beam ratios having the same forebody length^2–beam products are shown to have comparable propeller spray characteristics at the same gross loads.

Wind-tunnel tests of the series are described in reference 3 and indicate that the hull having a length–beam ratio of 15 had approximately 29 percent less aerodynamic drag than the hull having a length–beam ratio of 6.

The purpose of the present investigation was to determine the effect of length–beam ratio on propeller, flap, and tail spray in smooth water. All the data were obtained visually and are presented in the form of photographs showing the region in which spray was observed to strike propellers or flaps and vee diagrams showing gross load plotted against speed.

SYMBOLS

C_{Δ_o}	gross-load coefficient (Δ_o/wb^3)
Δ_o	gross load, pounds
V	speed, feet per second
w	specific weight of water, pounds per cubic foot (63.5 for this investigation)
δ_e	elevator deflection, degrees
δ_f	flap deflection, degrees
L/b	length–beam ratio
b	maximum beam, feet
$L = L_f + L_a$	
L_f	length of forebody from bow to step, feet
L_a	length of afterbody from step to sternpost, feet
L_f/b	forebody length–beam ratio
k	nondimensional coefficient relating forebody proportions to spray characteristics (Δ_o/wbL_f^2)

DESCRIPTION OF MODELS

Figure 1 is a drawing showing the general arrangements of the models superimposed one upon the other; figure 2 is a drawing showing typical sections of the forebodies. All models are $\frac{1}{10}$-size models of the same airplane incorporating the various hulls of the series. Table I gives the pertinent dimensions of the models.

The first model of the series was Langley tank model 203A, derived from the full-size Navy twin-engine flying boat. The nacelles, propellers, wing, and tail surfaces of model 203A correspond to those of the full-size flying boat and were placed in the same locations with respect to the step. The model hull dimensions were derived by increasing the length-beam ratio from 6.3, that of the full-size flying boat, to 9.0 while constant length^2-beam product was maintained. The same depth of hull and ratio of length of forebody to length of afterbody were used.

Langley tank models 213A, 214A, and 224A were derived from model 203A by varying the station spacings in proportion to the lengths while keeping the angle between forebody and afterbody keels constant. The cross sections below the chines were made geometrically similar and the deck radii were made equal to the chine half-breadth at each station thus derived. The nacelles, propellers, wing, and tail surfaces used for all models also corresponded to those of the full-size flying boat and were placed in the same locations with respect to the step. The resulting hulls are thus as closely related as possible over the wide range of length-beam ratio covered by the series and are interchangeable on the same over-all seaplane design for direct comparisons of their hydrodynamic characteristics.

The construction of the models was similar to that described in reference 4. In order to make the stall occur at angles more nearly equal to those estimated for the full-size wing, leading-edge slats were installed on the wing. Split flaps and three-blade propellers were used on all models.

Photographs of the models having length-beam ratios of 6 and 15 are shown in figure 3, and in these photographs may be seen the chine stations (inches forward of the step).

APPARATUS AND PROCEDURE

The tests were made in Langley tank no. 1 which is described in reference 5. The towing gear is described in reference 4. The models were free to trim and rise but were restrained in roll and yaw.

The thrust used throughout these tests represents approximately the thrust of the full-size flying boat. The propellers were operated at 4600 rpm with a blade angle of 14°.

Two positions of the center of gravity, 28 percent and 36 percent mean aerodynamic chord, were used for models 213A, 203A, and 214A; whereas one position, 28 percent mean aerodynamic chord, was used for model 224A. Throughout these tests the elevators and flaps were deflected -10° and 20°, respectively. The models were tested at loads ranging from 55 pounds to 95 pounds, corresponding to 55,000 pounds and 95,000 pounds (full size). All the data were obtained visually and are presented in the form of vee diagrams, which are plots of load against speed showing the region in which spray was observed to strike the propellers or flaps. These vee diagrams delineate two types of spray: light spray and blister spray. Blister spray is the relatively solid sheet of water coming off and upwards from the chine and moving aft as the model gains speed. All spray not considered blister spray is designated light spray and consists of isolated drops. Blister spray is the primary concern of this investigation because this type of spray is responsible for most cases of damage to flying-boat components. No attempt was made to measure the intensity of the propeller spray beyond distinguishing between light spray and blister spray.

Slowly accelerated runs $\left(\text{about } \frac{1}{4} \text{ ft/sec}^2\right)$ were made through the spray range; and the spray conditions about the propellers, flaps, and chine were noted at speed intervals of $\frac{1}{2}$ foot per second. The trim was visually read at these intervals. The position along the chine of the leading edge of the main spray blister, gross loads, and the speeds at which heavy spray first entered the propeller disk were carefully determined for each model.

Motion pictures of the models at gross loads of 55, 65, 75, 85, and 95 pounds with accelerations of 2 feet per second per second for the center-of-gravity position of 28 percent mean aerodynamic chord were taken for detailed study of the spray. Photographs comparing the spray of the models at various speeds were also taken for inclusion in this paper.

RESULTS

Figures 4 to 10 show, for the center-of-gravity positions of 28 percent and 36 percent mean aerodynamic chord, the vee diagrams for spray in the propellers and flaps. Also shown in these figures are the trim variation and the position along the chine of the leading edge of the main spray blister. The regions of loads and speeds at which light spray and blister spray strike the propellers and flaps are enclosed by the dashed and solid lines, respectively. The position along the chine of the leading edge of the main spray blister was taken as the point of origin of the wave forming the blister measured in inches forward of the step.

Figure 11 is a comparison of the data of figures 4 to 10 and shows the blister-spray range with various length-beam ratios.

Figure 12 shows the variation of trim and leading edge of blister with length–beam ratio for a 75–pound gross load and a center–of–gravity position of 28 percent mean aerodynamic chord. Figures 13 and 14 are photographs of the spray for the models having length–beam ratios of 9 to 15 at various gross loads and speeds.

DISCUSSION

Spray in propellers.– Reference 1 indicates that hulls having the same values of L_f^2b will have similar spray characteristics for a given load. This conclusion was arrived at by a consideration of the spray characteristics of actual flying boats as reported by operational and maintenance personnel. A plot of load coefficient C_{Δ_o} against L_f/b yielded the relationship $k = \frac{\Delta_o}{wbL_f^2}$ where k may be considered a spray criterion ranging in value from 0.0525 for light spray to 0.0975 for excessive spray.

Since the models have the same values of L^2b and L_f^2b, they have identical k–values at the same loads and thus would be expected to have similar propeller spray characteristics. The observed spray characteristics of the models agree quite well with the designations of k–values as set forth in reference 1 and shown in figure 15. The photographs of figure 13 confirm the fact that the propeller spray characteristics are quite similar.

Of especial interest is the gross load and speed at which the blister spray first strikes the propellers as represented by the lower apex of the vee diagrams of figures 4 to 10. The C_{Δ_o}–values corresponding to these points are plotted in figure 15 for each of the models and the points fall in the region designated as light or satisfactory spray; the type of spray was confirmed by observations made during the tests.

Figure 11 indicates that model 213A $\left(\frac{L}{b} = 6\right)$ encounters propeller spray at lighter loads than do the models of higher length–beam ratio $\left(\frac{L}{b} = 9, 12, \text{ and } 15\right)$. Since this model represents a conventional length–beam–ratio configuration of a flying–boat hull, the test indicates that models of higher length–beam ratios offer some advantage in this respect. The position of the lower apex of the blister–spray vee diagram as plotted in figure 15 supports the fact that the spray criterion in reference 1 may be considered conservative for hulls with high length–beam ratios, based on the load at which spray first enters the propellers at low length–beam ratios.

The procedure of varying length–beam ratio while holding L^2b and L_f^2b constant, therefore, yields a series of hulls having approximately similar spray characteristics.

Spray on flaps.– The vee diagrams for flap spray, figures 4 to 11, define the range of speed and load over which the flaps are subjected to spray. In the case of light spray it is quite difficult to define the origin, that is, to differentiate between spray thrown directly astern and against the flaps by the propellers and spray blown by the propeller slipstream against the under side of the wing. When blown by the propeller slipstream, the water is deposited on the under side of the wing in the forward area. The water follows the wing contour aft to the flaps and finally leaves the trailing edge as spray. This light spray on the flaps does not appear to be of a severe or destructive nature.

Blister spray, however, may be of a destructive nature. This type of spray occurs when the main blister or wave resulting from the hull passage through the water reaches the region of the flaps and is high enough to impinge directly against them as shown by the photographs of figure 14. This type of spray is known to induce relatively large loads on the flaps or, in the absence of flaps, on the trailing edge of the wing. Figures 4 to 9 for the two center–of–gravity positions indicate that this spray is not appreciably affected by trim. Observations made during the test and studies of the photographs of figure 14 disclosed no variation of flap–spray intensity among the various models at high loads, but a study of the vee diagrams shows that use of high length–beam ratios slightly increases the range of speed over which the flaps are subjected to spray. This increase may be caused by the fact that the models with high length–beam ratios have greater drafts throughout the take–off runs. Also of interest is the fact that the spanwise areas of the flaps subject to blister spray were very nearly the same in all the models.

At light loads (55 to 65 lb) the models with high length–beam ratios have a slight advantage in that they carried a greater load without blister spray occurring on the flaps. (See fig. 11.)

Spray on elevators.– The speeds at which tail spray appears most severe are beyond the speed range of the photographs of figure 14. Supplementary observations, however, indicated that blister spray striking the elevators was more severe for the models having high length–beam ratios. Preventative measures such as spray strips and chine flare may be used to control the spray striking the propellers, but there appears to be no way of preventing the spray from striking the elevators other than placing them higher.

Trim and position of blister.– Figure 11 shows that changing the position of the center of gravity had no appreciable effect on the

blister spray range of the models, although trim was affected. Figure 12 shows that, for a gross load of 75 pounds, no abrupt changes occurred in the trim or the position along the chine of the leading edge of the main spray blister that might be ascribed to changes in length–beam ratio.

CONCLUSIONS

An investigation, made in Langley tank no. 1, of the spray characteristics in smooth water of four related flying-boat-hull models having length–beam ratios of 6, 9, 12, and 15 and constant values of length^2–beam product indicated the following conclusions:

1. Designers wishing to take advantage of the higher length–beam ratios of the series in order to achieve better aerodynamic performance may do so without fear of appreciably penalizing the spray characteristics in smooth water.

2. When forebody length^2–beam product was held constant, similar propeller and flap spray characteristics were obtained for hulls over a very wide range of length–beam ratio; however, higher length–beam ratios may require greater clearance between elevators and water.

3. The spray characteristics of the models agreed quite well with the spray criterion presented in NACA ARR No. 3K08. This criterion may be considered conservative for hulls with high length–beam ratios as shown by the fact that the models having length–beam ratios of 9, 12, and 15 operated at greater loads with no propeller spray than did the model having the more conventional length–beam ratio of 6.

4. Trim changes, introduced by changing the center-of-gravity position from 28 percent to 36 percent mean aerodynamic chord, had no appreciable effect on the spray characteristics.

Langley Aeronautical Laboratory
National Advisory Committee for Aeronautics
Langley Field, Va., June 1, 1948

REFERENCES

1. Parkinson, John B.: Design Criterions for the Dimensions of the Forebody of a Long-Range Flying Boat. NACA ARR No. 3K08, 1943.

2. Land, Norman S., Bidwell, Jerold M., and Goldenbaum, David M.: The Resistance of Three Series of Flying-Boat Hulls as Affected by Length-Beam Ratio. NACA ARR No. L5G23, 1945.

3. Yates, Campbell C., and Riebe, John M.: Effect of Length-Beam Ratio on the Aerodynamic Characteristics of Flying-Boat Hulls. NACA TN No. 1305, 1947.

4. Olson, Roland E., and Land, Norman S.: Methods Used in the NACA Tank for the Investigation of the Longitudinal-Stability Characteristics of Models of Flying Boats. NACA Rep. No. 753, 1943.

5. Truscott, Starr: The Enlarged N.A.C.A. Tank, and Some of Its Work. NACA TM No. 918, 1939.

TABLE I

PERTINENT DIMENSIONS OF MODELS

[Depth of step (percent b), 9; k = 0.069 for design gross load of 65 lb]

Model	L/b	L_f/b	Over-all length (in.)	L_f	L_a	b	Hull volume (cu in.) (a)	Design C_{Δ_o}
213A	6	3.45	110.19	44.58	32.87	12.91	14,860	0.82
203A	9	5.18	116.65	51.04	37.64	9.85	12,910	1.85
214A	12	6.91	121.78	56.17	41.42	8.13	11,520	3.29
224A	15	8.63	126.12	60.51	44.64	7.01	10,650	5.15

[a]Approximate values given.

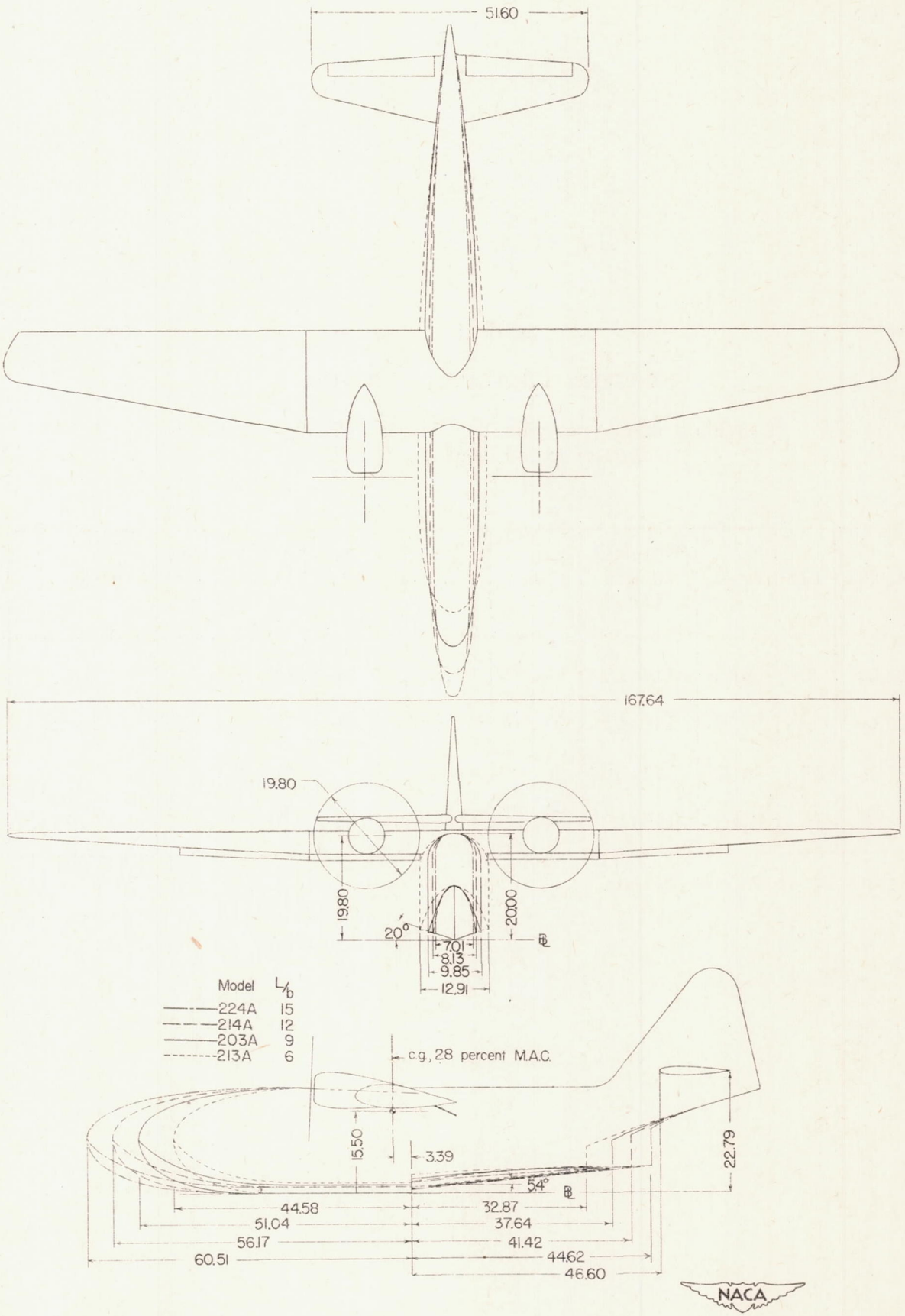

Figure 1.– General arrangement of Langley tank models having four different length-beam ratios. (Dimensions in inches.)

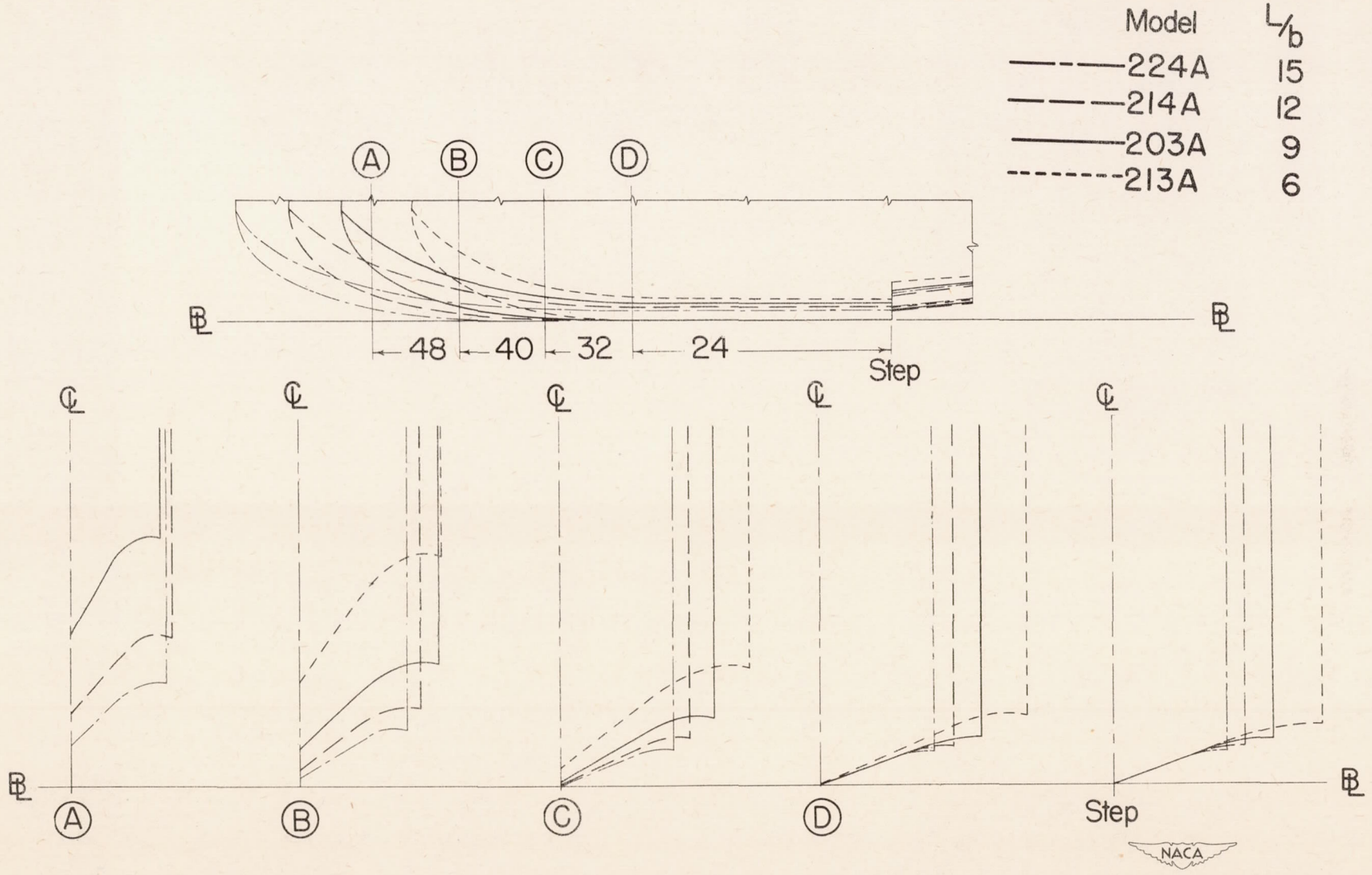

Figure 2.- Comparison of hull sections of Langley tank models having four different length-beam ratios. (Dimensions in inches.)

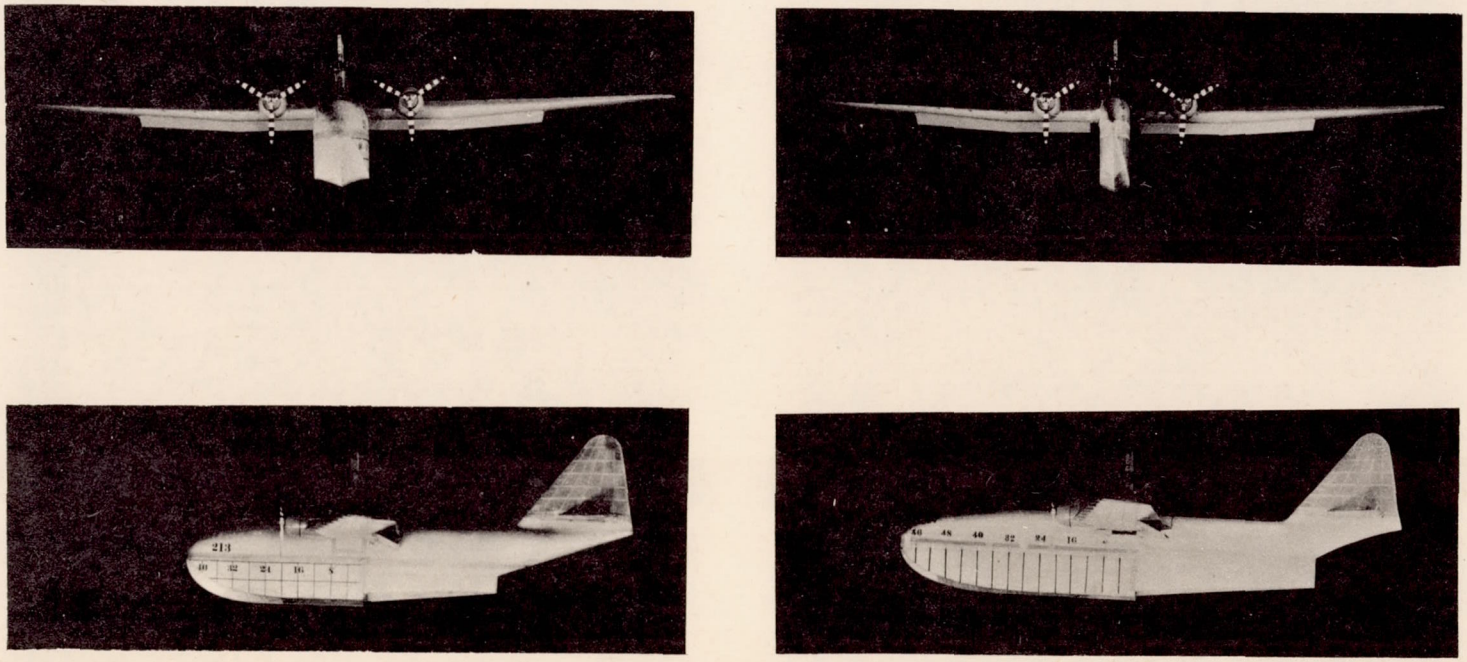

(a) Model 213; L/b, 6.

(b) Model 224; L/b, 15.

Figure 3.- Front and side views of two Langley tank models having length-beam ratios of 6 and 15.

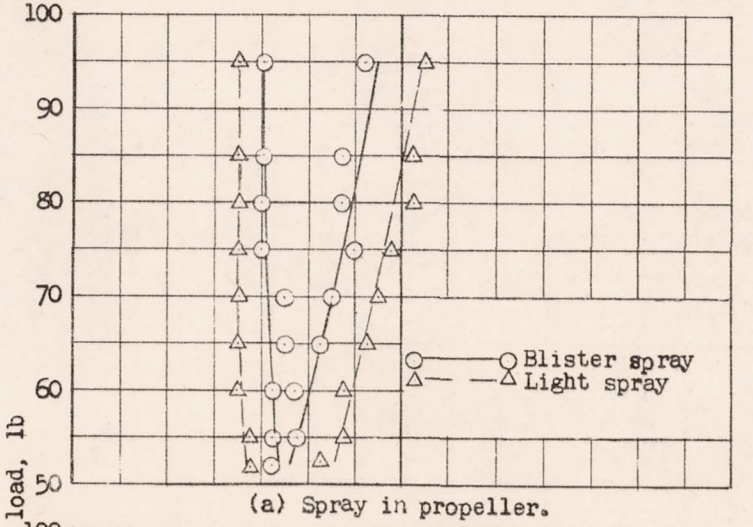

(a) Spray in propeller.

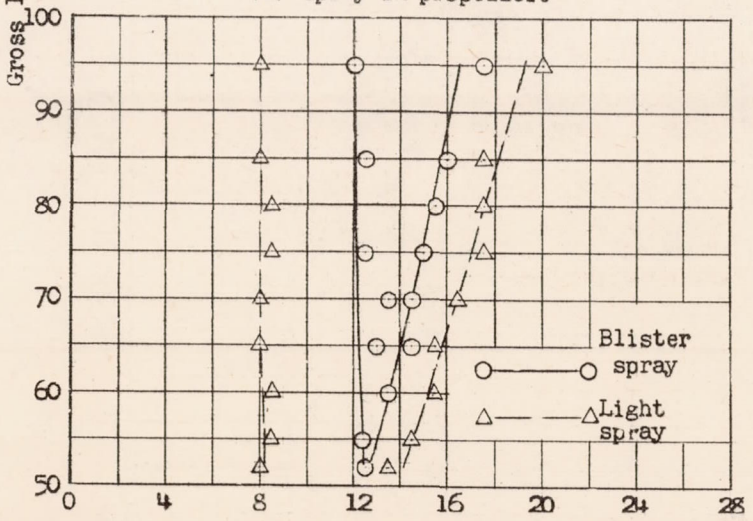

Speed, fps

(b) Spray on flaps.

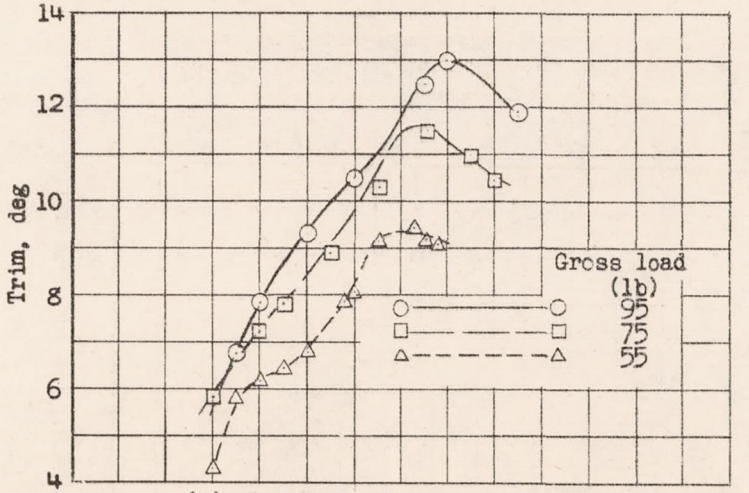

(c) Variation of trim with speed.

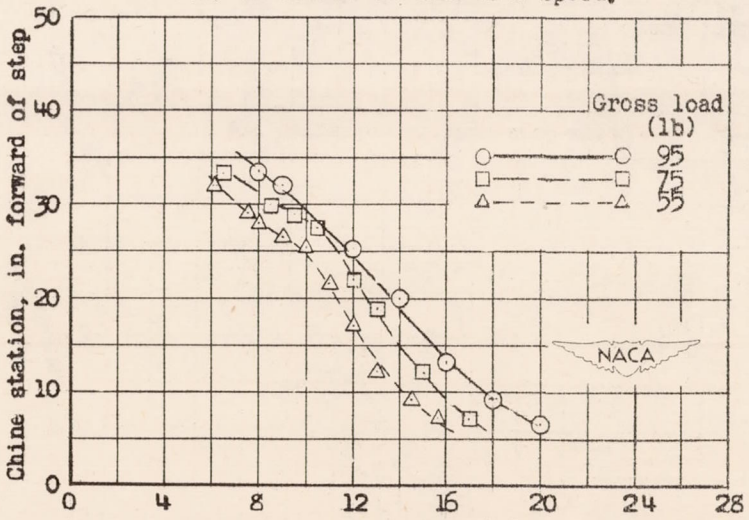

Speed, fps

(d) Variation of leading edge of blister at chine with speed.

Figure 4.- Spray and trim characteristics of model 213A. L/b, 6; center of gravity, 28 percent mean aerodynamic chord; δ_f, 20°; δ_e, -10°.

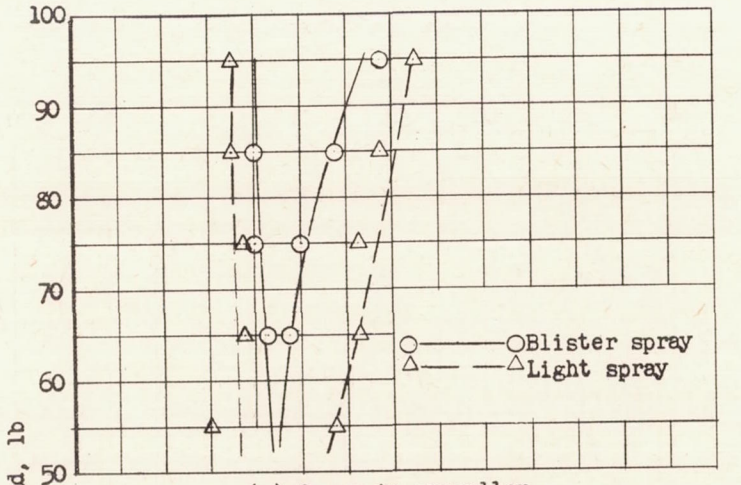

(a) Spray in propeller.

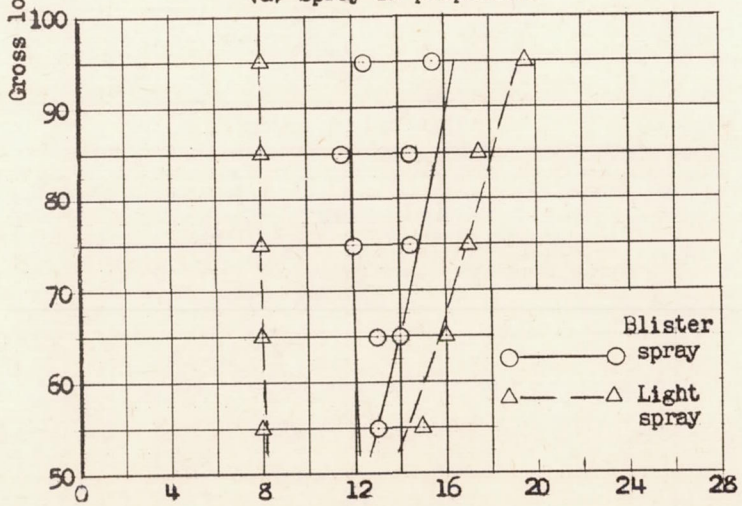

(b) Spray on flaps.

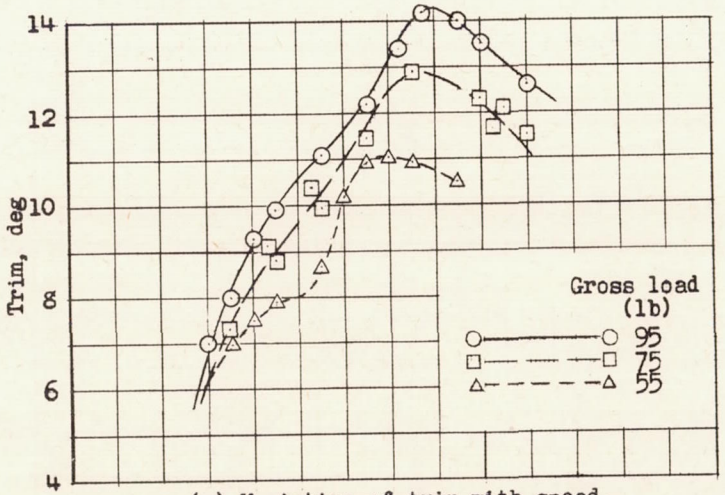

(c) Variation of trim with speed.

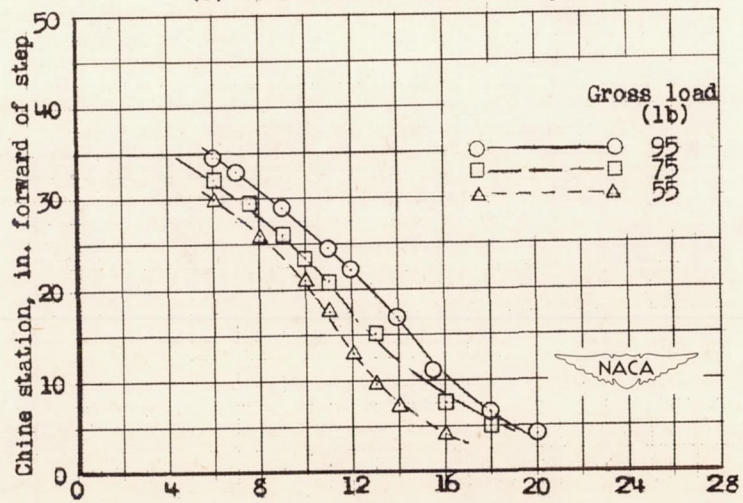

(d) Variation of leading edge of blister at chine with speed.

Figure 5.– Spray and trim characteristics of model 213A. L/b, 6; center of gravity, 36 percent mean aerodynamic chord; δ_f, 20°; δ_e, −10°.

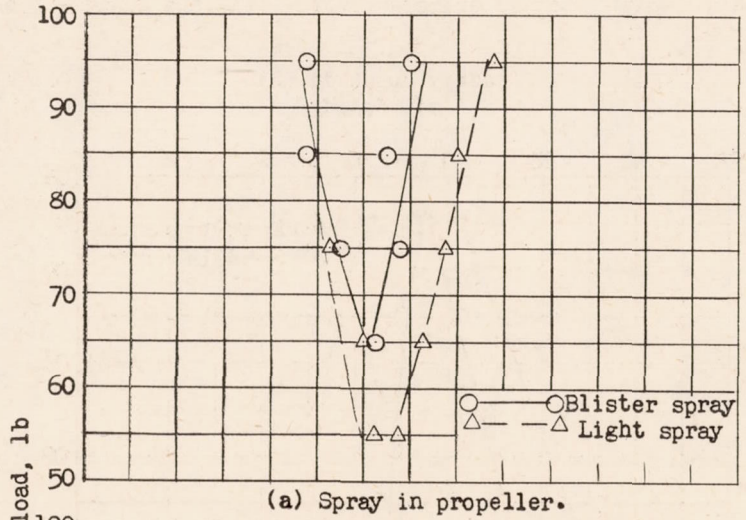

(a) Spray in propeller.

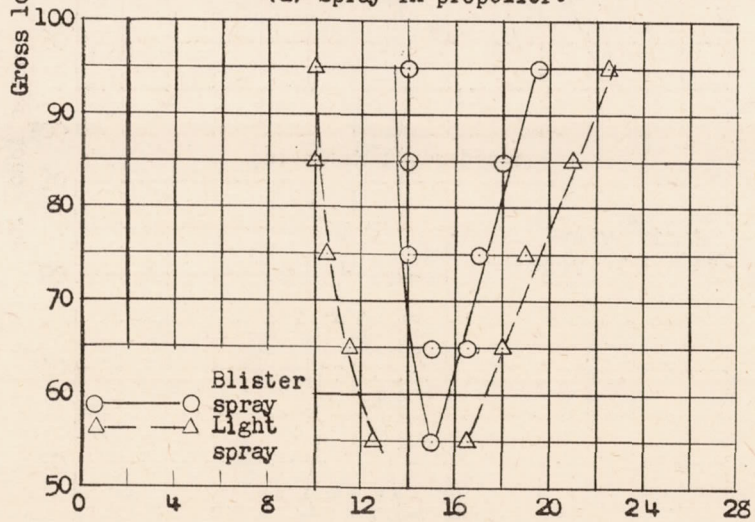

Speed, fps
(b) Spray on flaps.

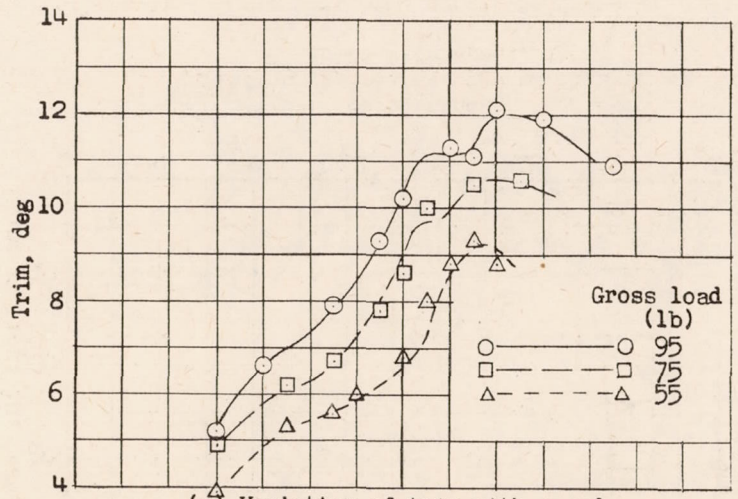

(c) Variation of trim with speed.

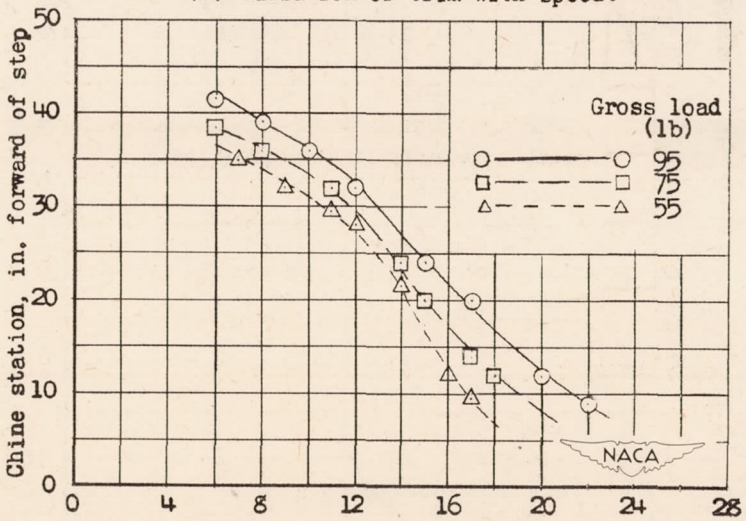

Speed, fps
(d) Variation of leading edge of blister at chine with speed.

Figure 6.- Spray and trim characteristics of model 203A. L/b, 9; center of gravity, 28 percent mean aerodynamic chord; δ_f, 20°; δ_e, -10°.

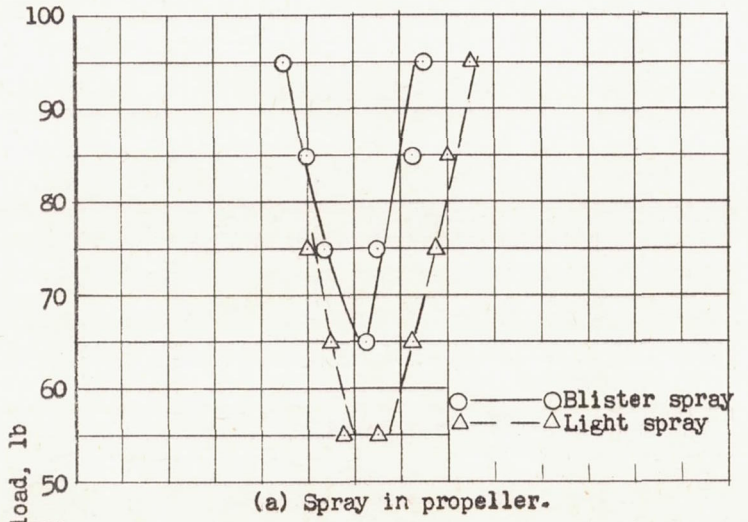

(a) Spray in propeller.

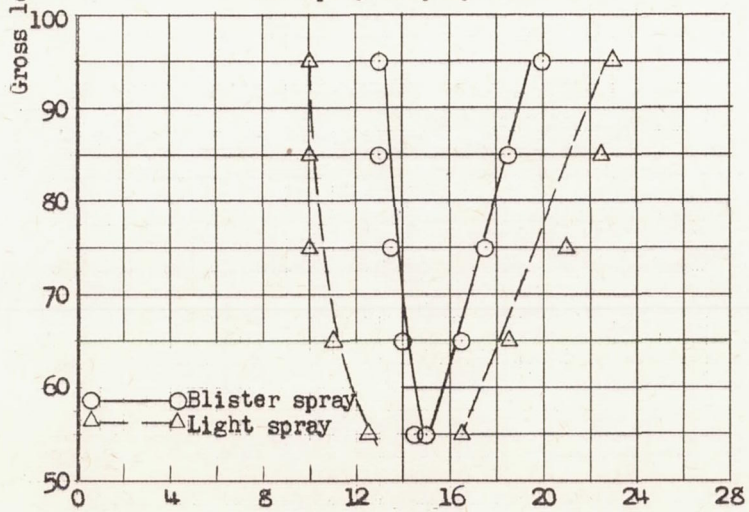

(b) Spray on flaps.

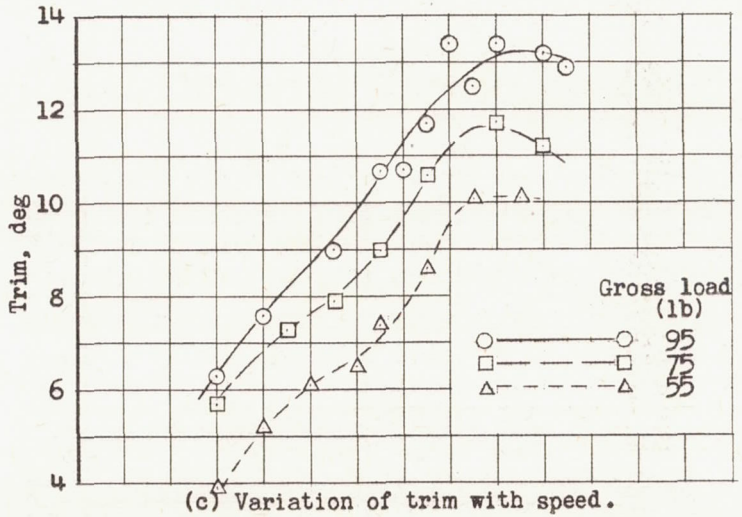

(c) Variation of trim with speed.

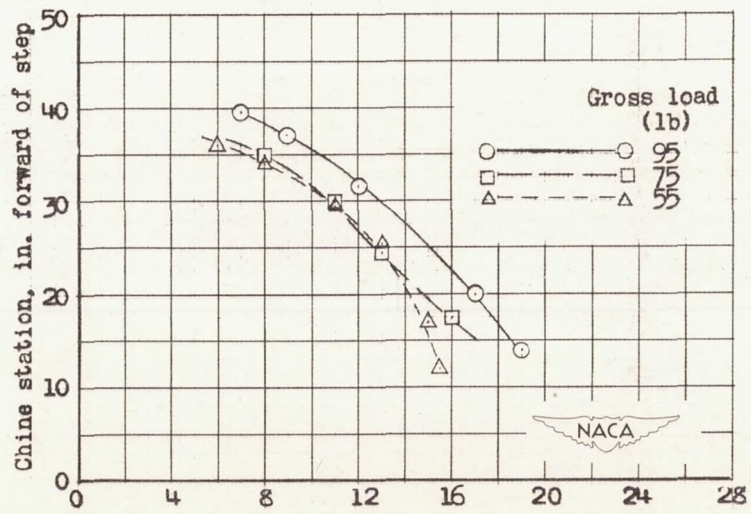

(d) Variation of leading edge of blister at chine with speed.

Figure 7.- Spray and trim characteristics of model 203A. L/b, 9; center of gravity, 36 percent mean aerodynamic chord; δ_f, 20°; δ_e, -10°.

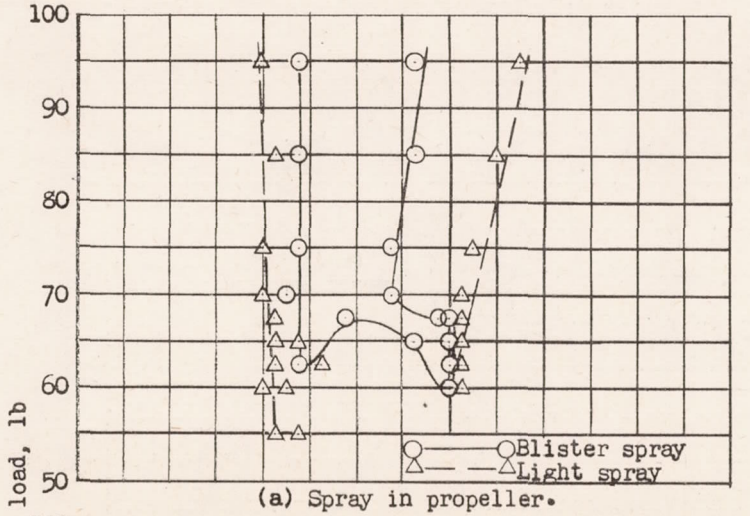

(a) Spray in propeller.

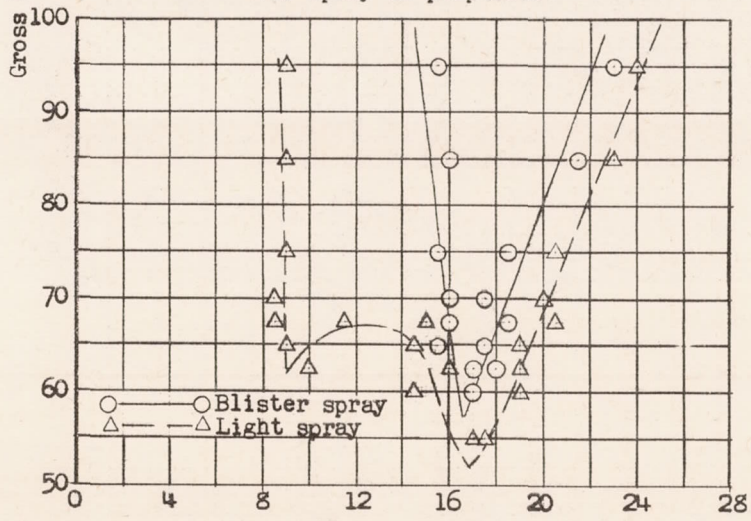

(b) Spray on flaps.

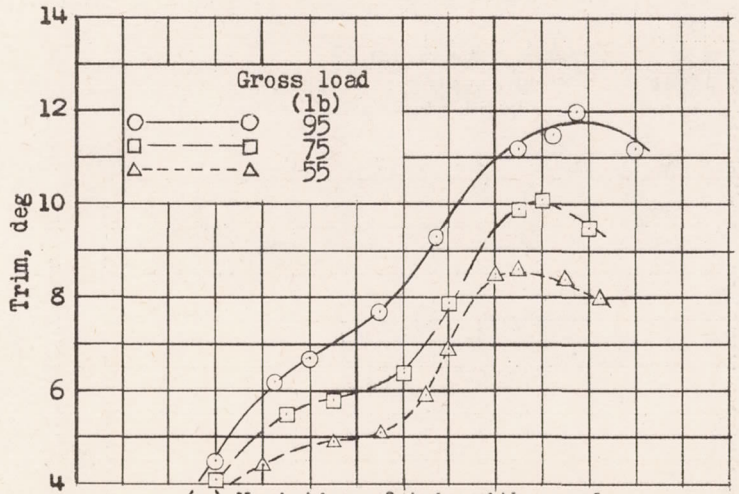

(c) Variation of trim with speed.

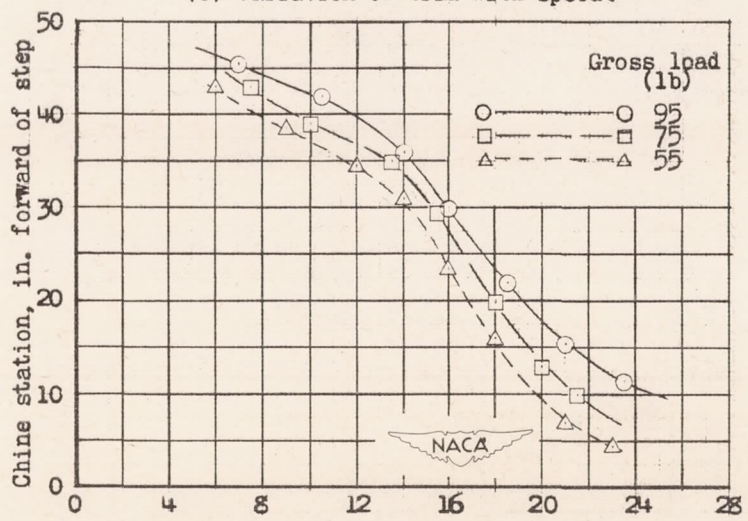

(d) Variation of leading edge of blister at chine with speed.

Figure 8.- Spray and trim characteristics of model 214A. L/b, 12; center of gravity, 28 percent mean aerodynamic chord; δ_f, 20°; δ_e, -10°.

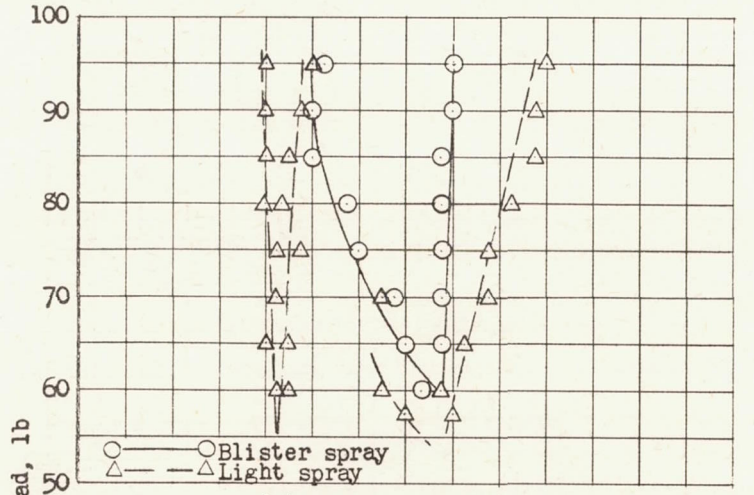

(a) Spray in propeller.

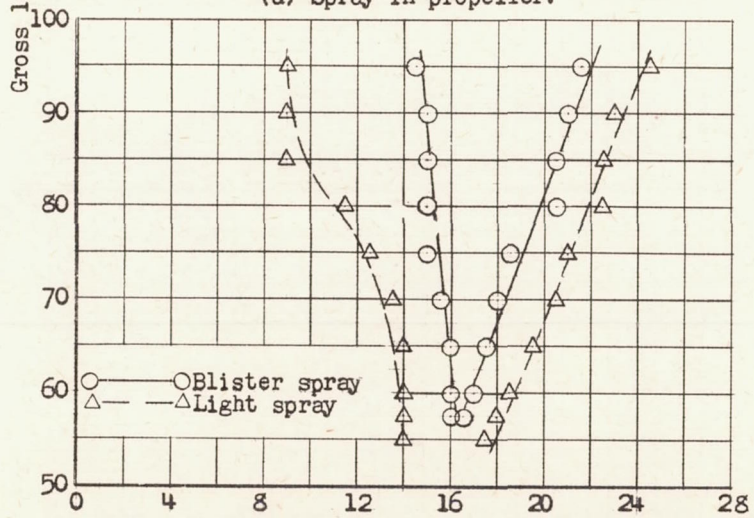

(b) Spray on flaps.

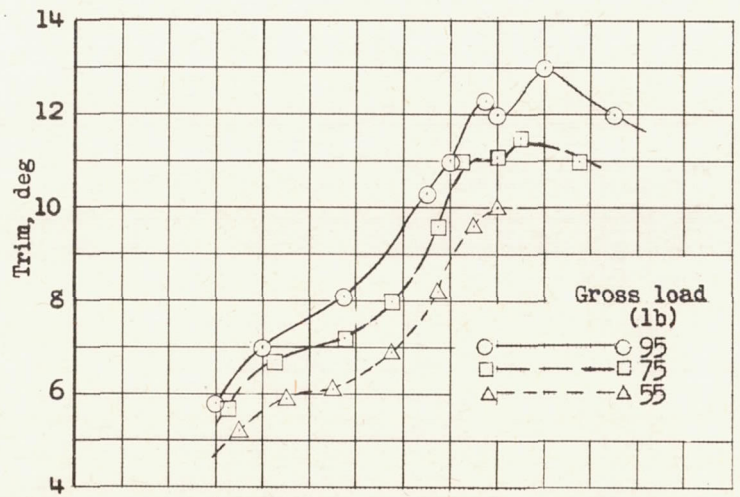

(c) Variation of trim with speed.

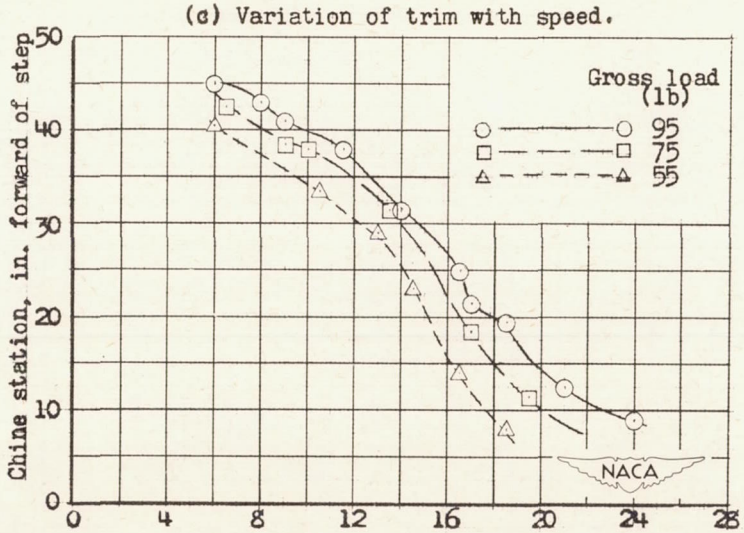

(d) Variation of leading edge of blister at chine with speed.

Figure 9.- Spray and trim characteristics of model 214A. L/b, 12; center of gravity, 36 percent mean aerodynamic chord; δ_f, 20°; δ_e, -10°.

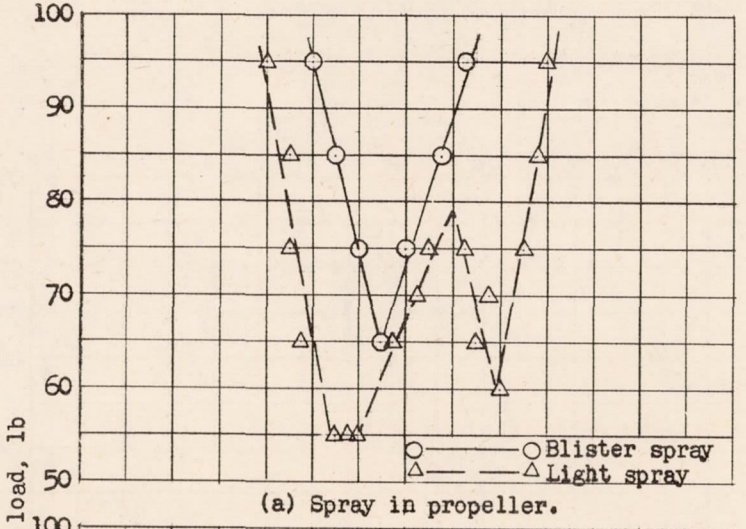

(a) Spray in propeller.

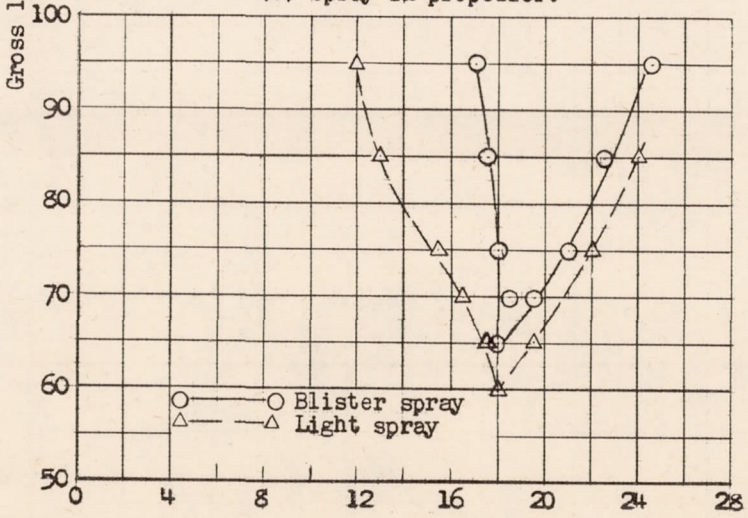

Speed, fps
(b) Spray on flaps.

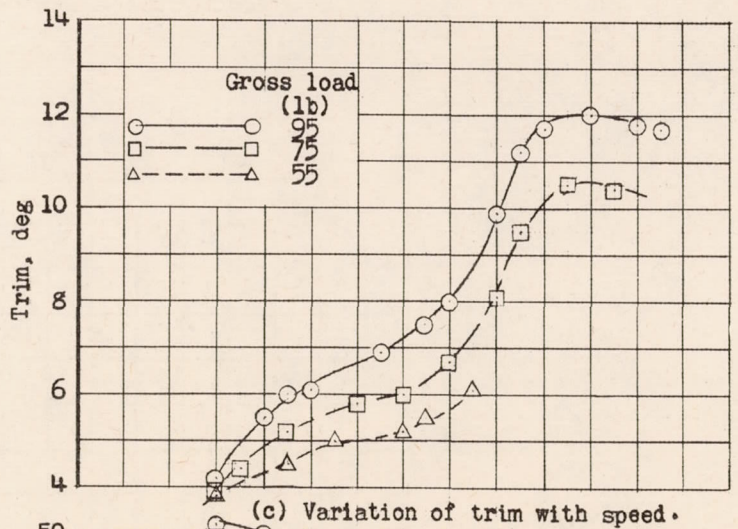

(c) Variation of trim with speed.

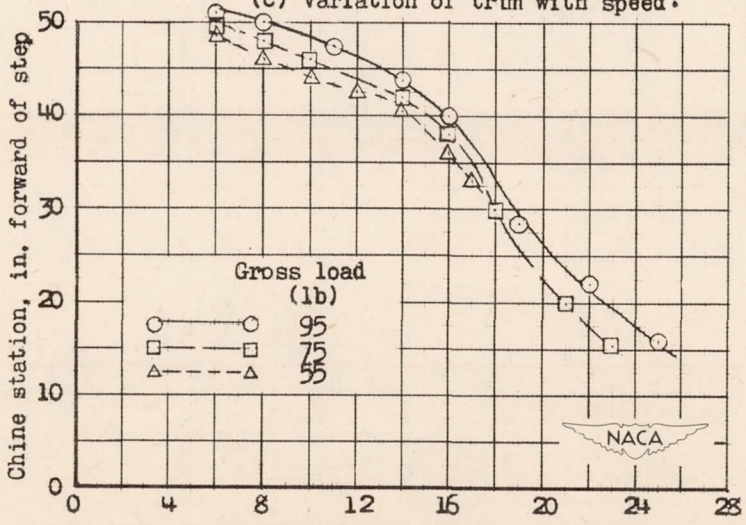

Speed, fps
(d) Variation of leading edge of blister a chine with speed.

Figure 10.- Spray and trim characteristics of model 224A. L/b, 15; center of gravity, 28 percent mean aerodynamic chord δ_f, 20°; δ_e, -10°.

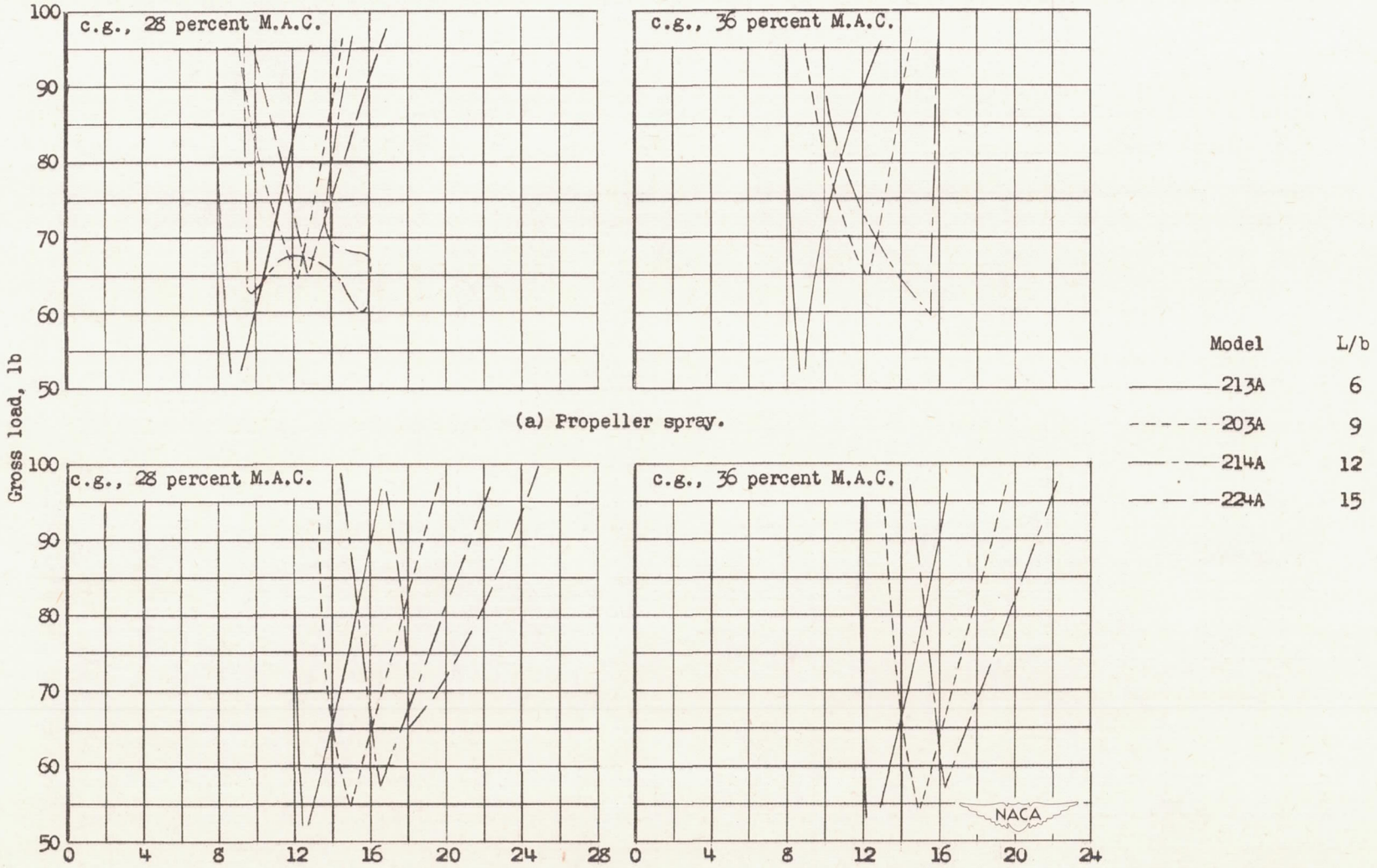

(a) Propeller spray.

(b) Flap spray.

Figure 11.– Blister spray range with various length–beam ratios.

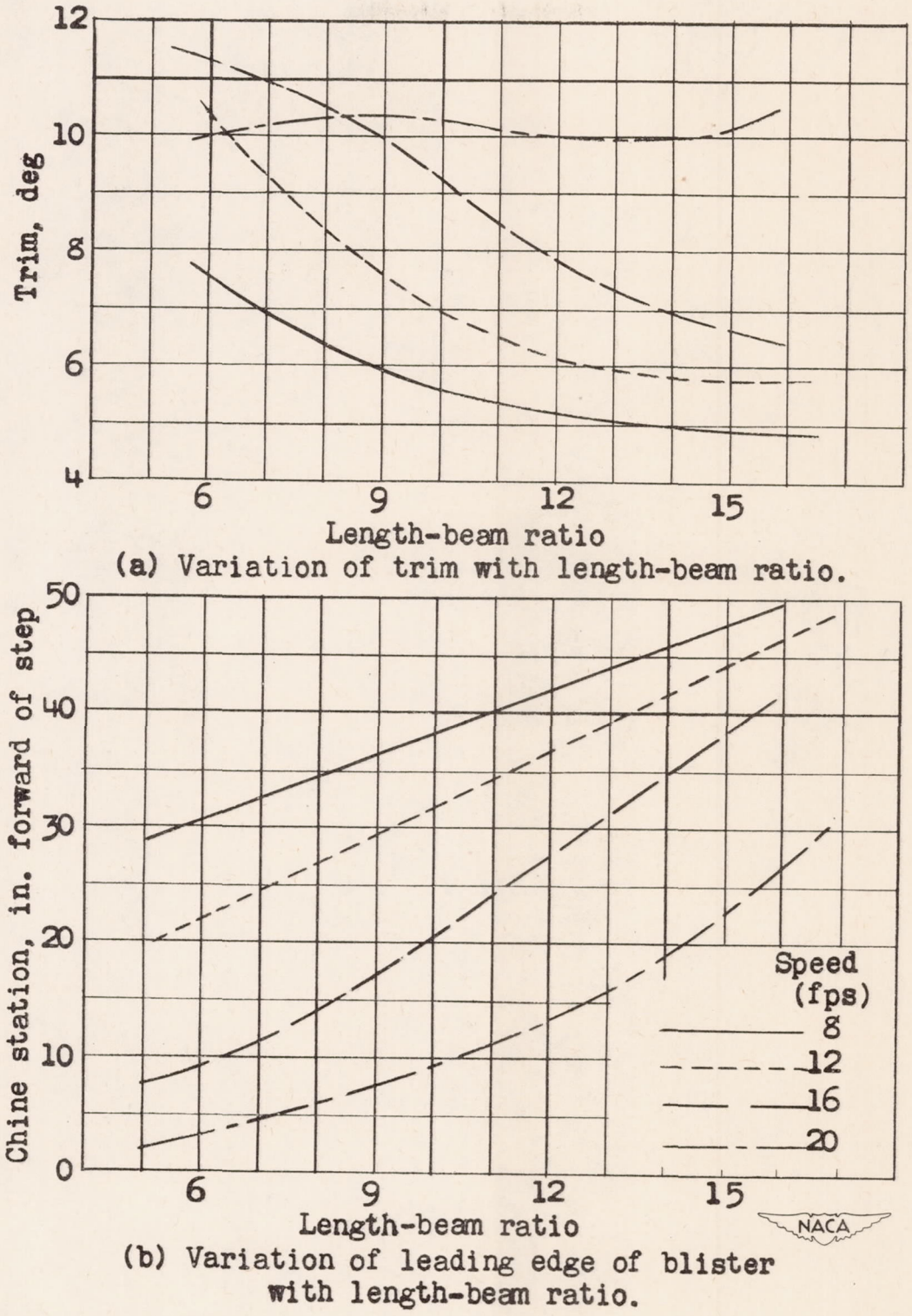

Figure 12.- Variation of trim and leading edge of blister with length-beam ratio. Center of gravity, 28 percent mean aerodynamic chord; gross load, 75 pounds; δ_f, 20°; δ_e, -10°.

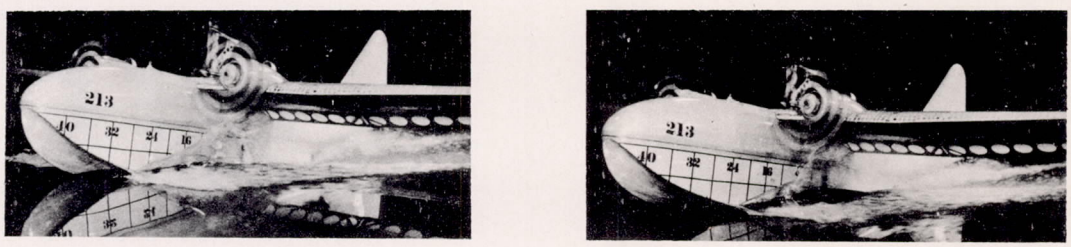

L/b, 6

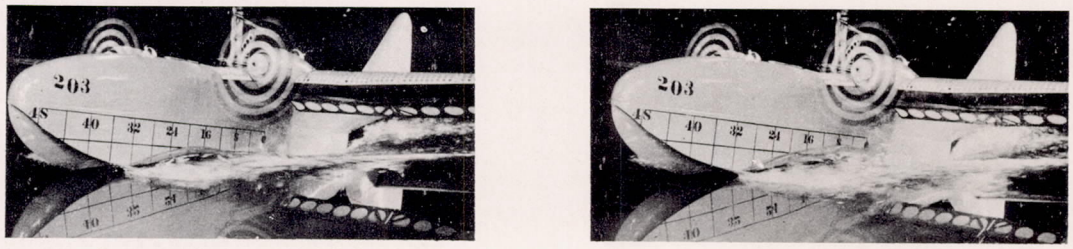

L/b, 9

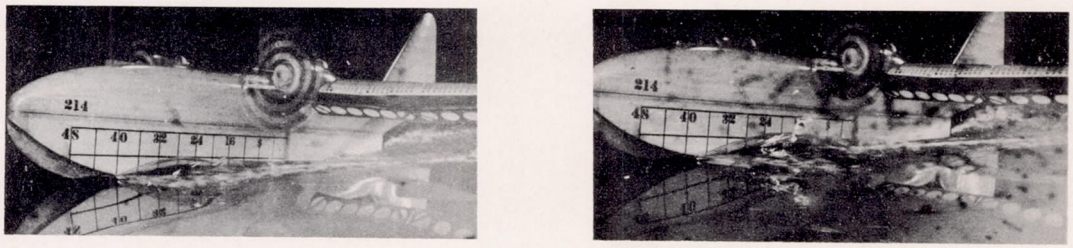

L/b, 12

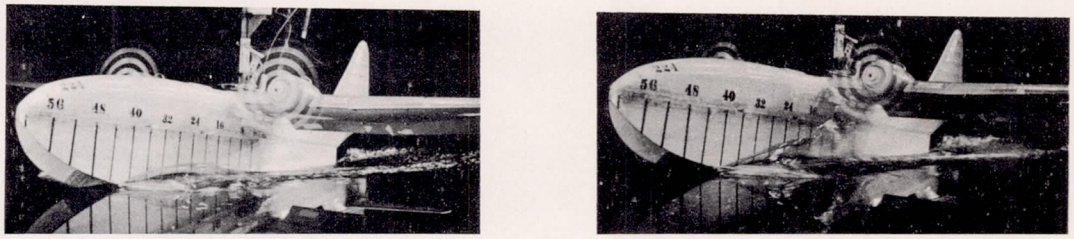

L/b, 15

V, 9.0 fps V, 11.0 fps

NACA

(a) Gross load, 65 pounds.

Figure 13.- Bow spray. Center of gravity, 28 percent mean aerodynamic chord; $\delta_f = 20^\circ$; $\delta_e = -10^\circ$.

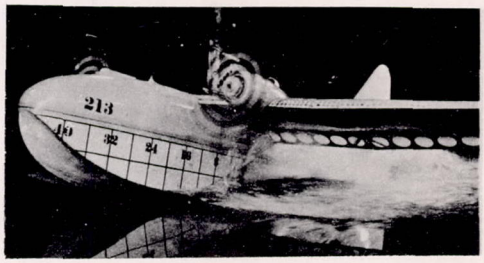

L/b, 6

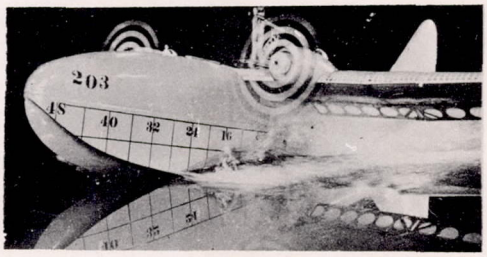

L/b, 9

L/b, 12

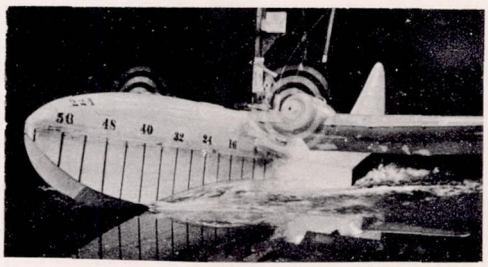

L/b, 15
V, 13.0 fps

(a) Concluded.

Figure 13.- Continued.

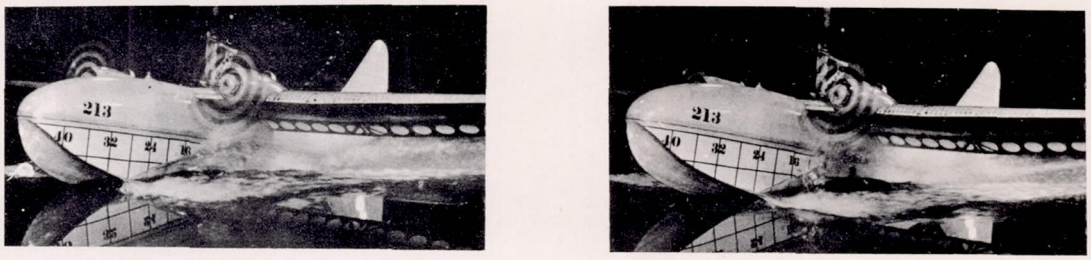

L/b, 6

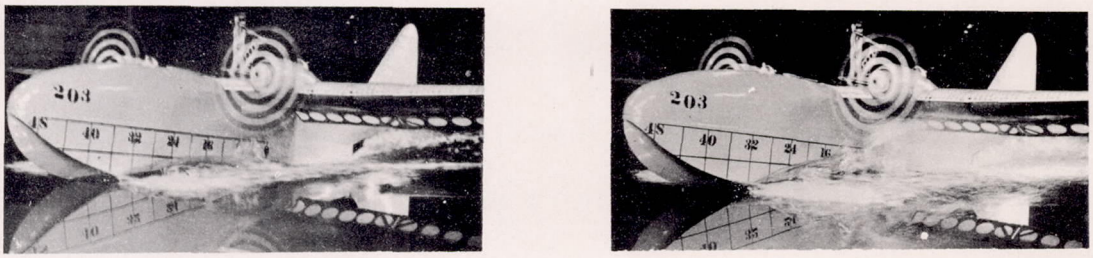

L/b, 9

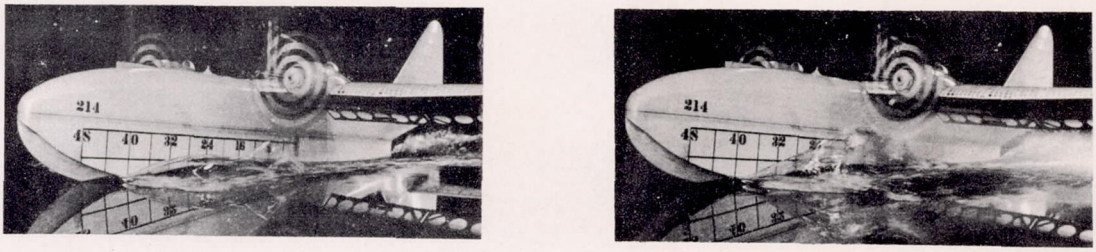

L/b, 12

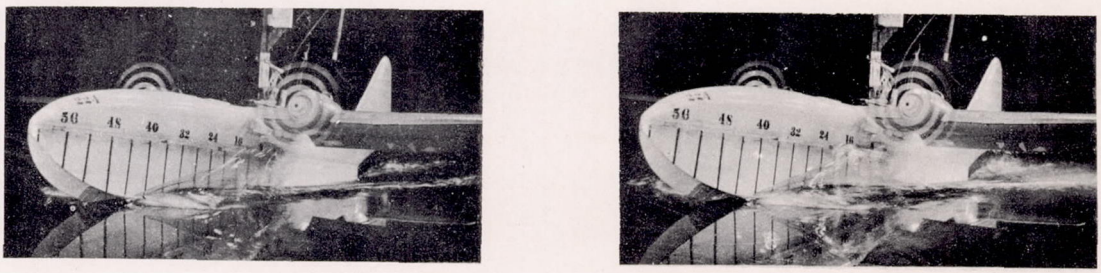

V, 9.0 fps L/b, 15 V, 11.0 fps

(b) Gross load, 75 pounds.

Figure 13.- Continued.

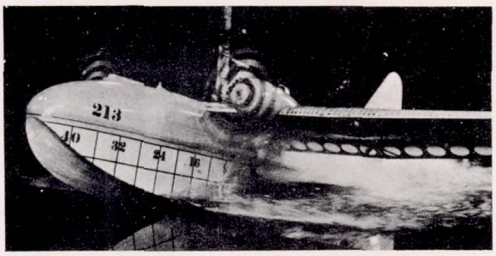

L/b, 6

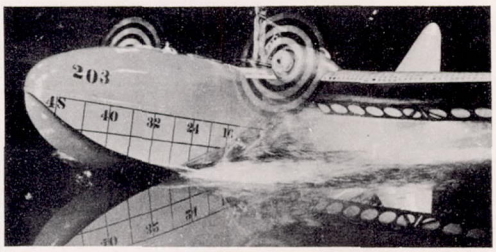

L/b, 9

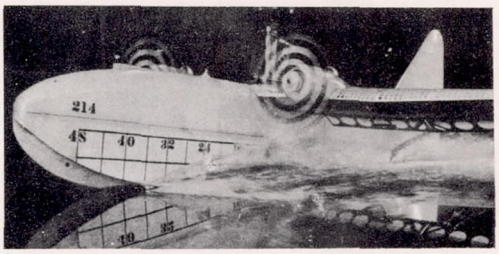

L/b, 12

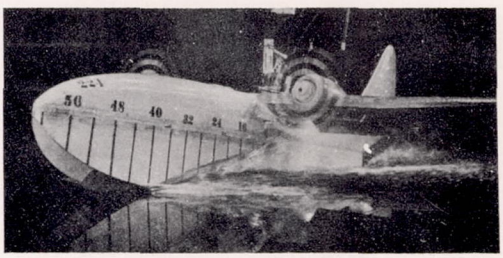

L/b, 15
V, 13.0 fps

(b) Concluded.

Figure 13.- Continued.

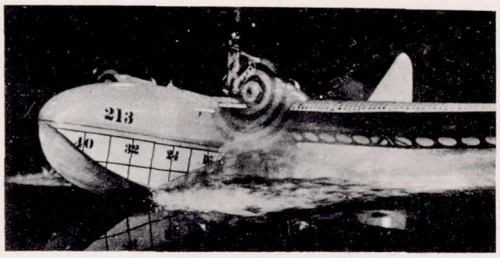

L/b, 6

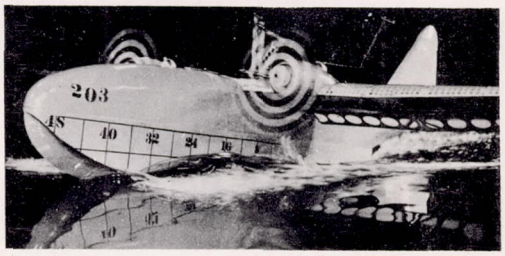

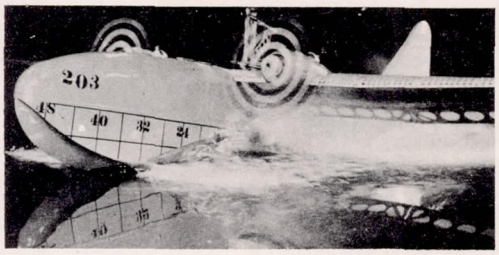

L/b, 9

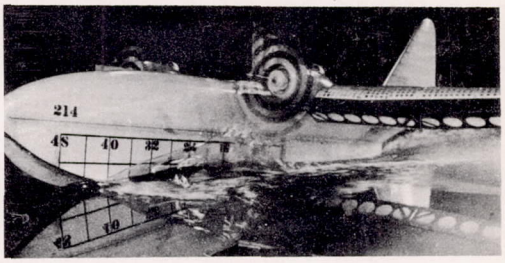

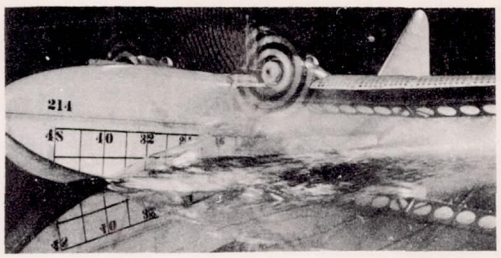

L/b, 12

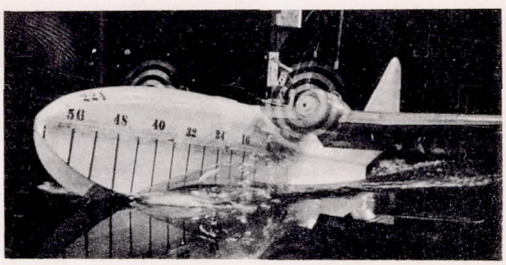

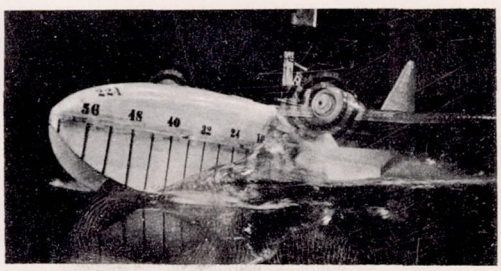

L/b, 15

V, 9.0 fps

V, 11.0 fps

(c) Gross load, 85 pounds.

Figure 13.- Continued.

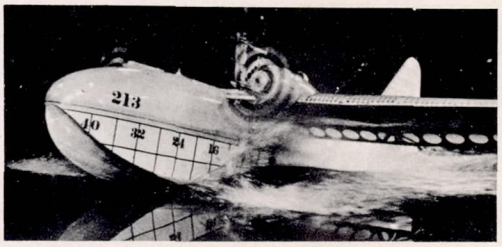

L/b, 6

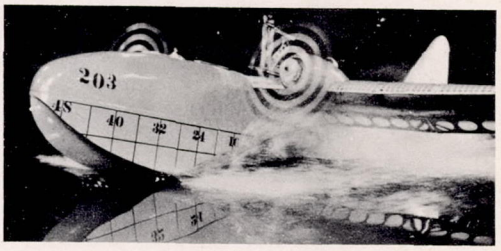

L/b, 9

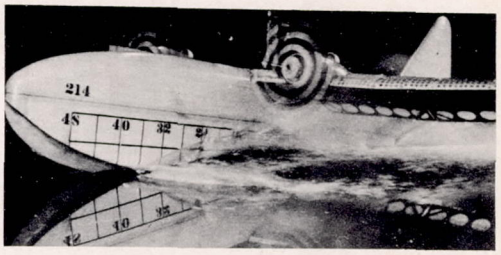

L/b, 12

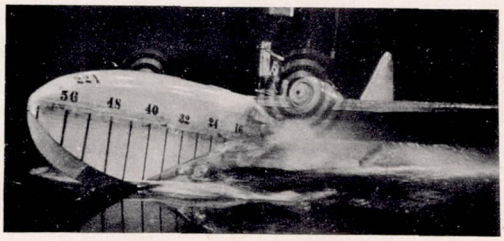

L/b, 15
V, 13.0 fps

(c) Concluded.

Figure 13.- Concluded.

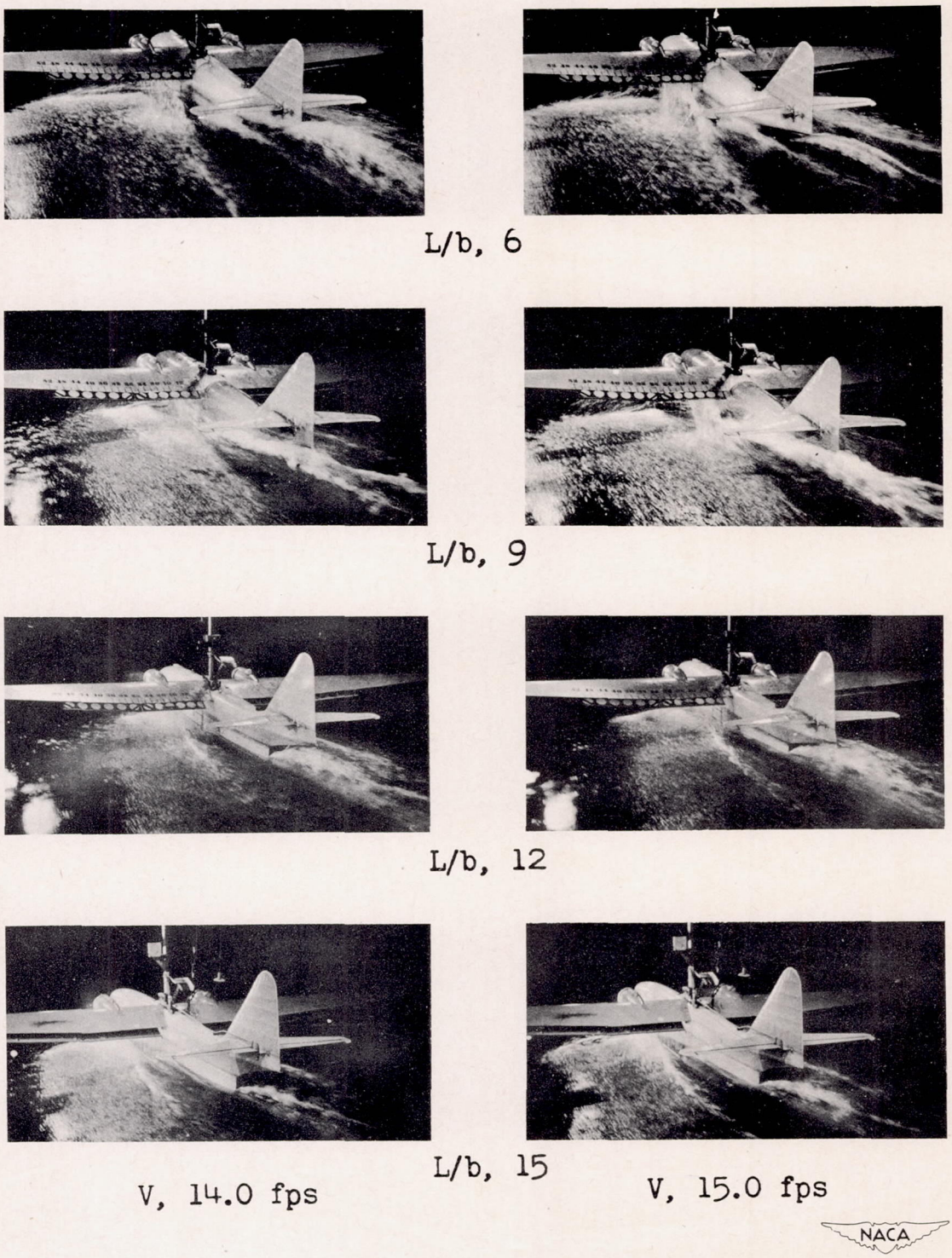

(a) Gross load, 75 pounds.

Figure 14.- Tail spray. Center of gravity, 28 percent mean aerodynamic chord; δ_f, 20°; δ_e, -10°.

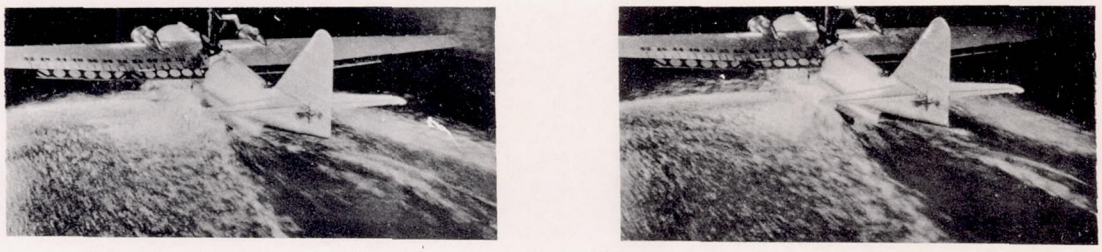

L/b, 6

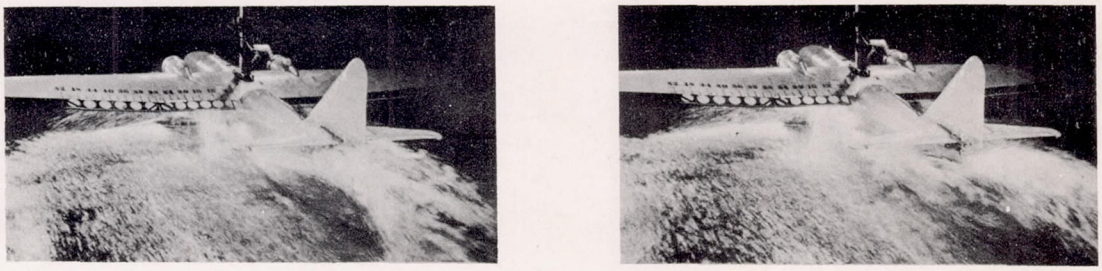

L/b, 9

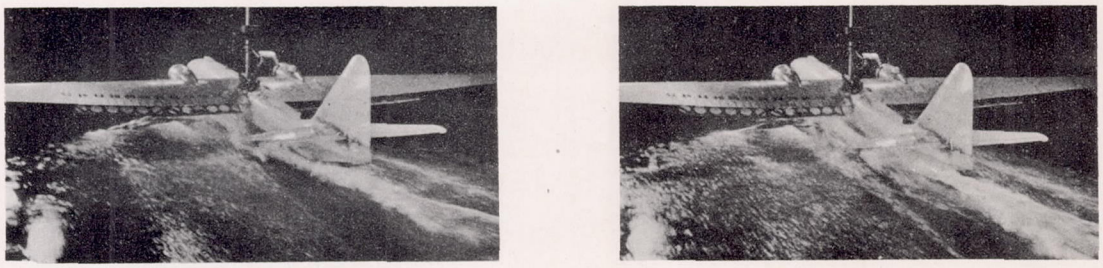

L/b, 12

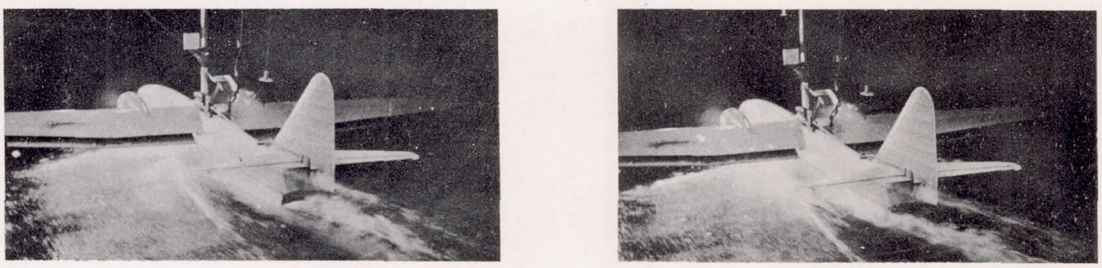

V, 16.0 fps L/b, 15 V, 17,0 fps

NACA

(a) Continued.

Figure 14.- Continued.

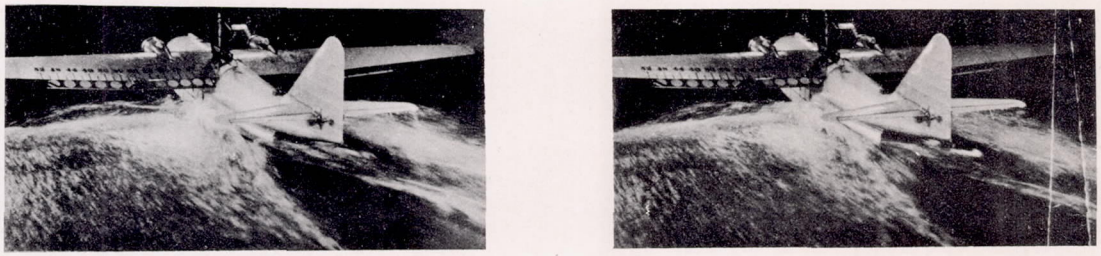

L/b, 6

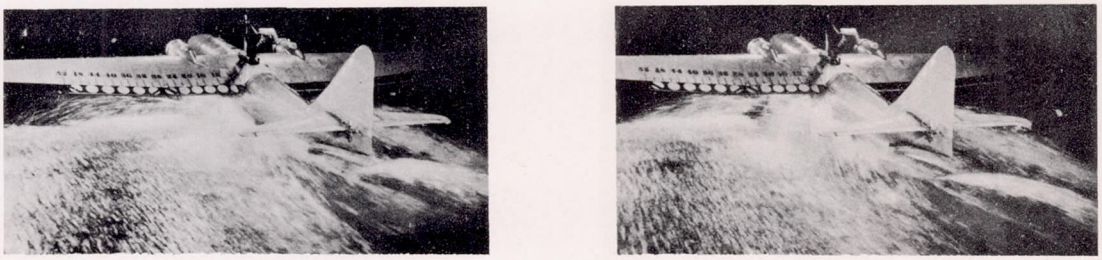

L/b, 9

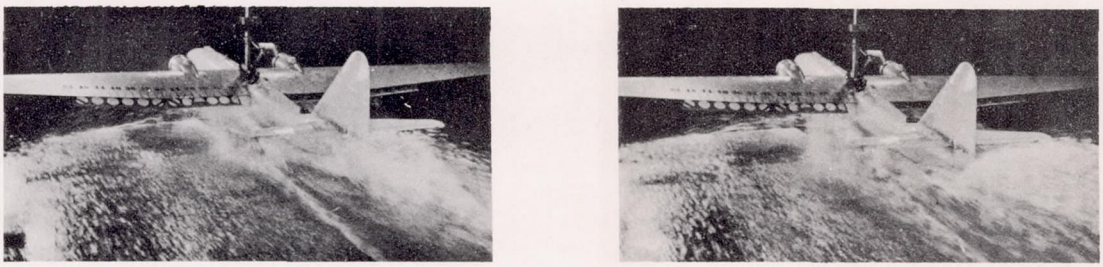

L/b, 12

L/b, 15

V, 18.0 fps V, 19.0 fps

NACA

(a) Concluded.

Figure 14.- Continued.

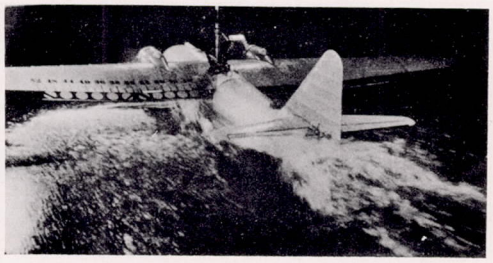

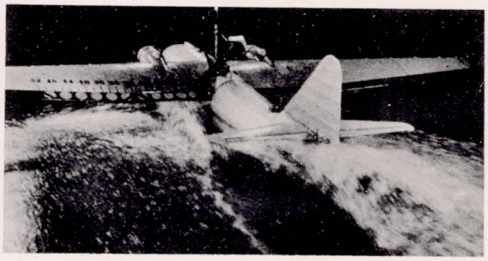

L/b, 6

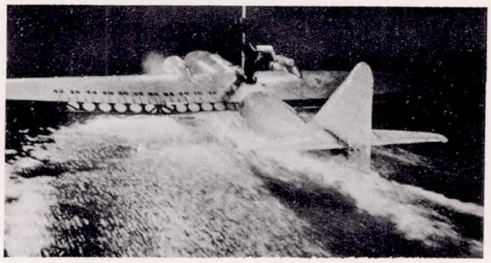

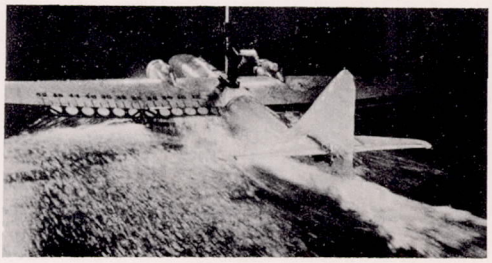

L/b, 9

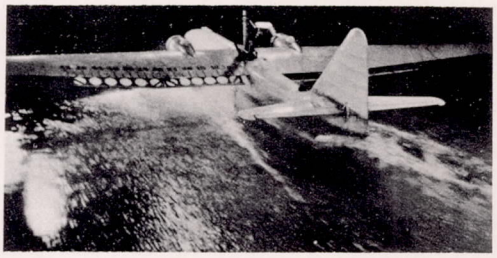

L/b, 12

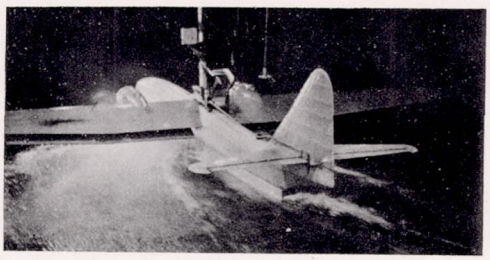

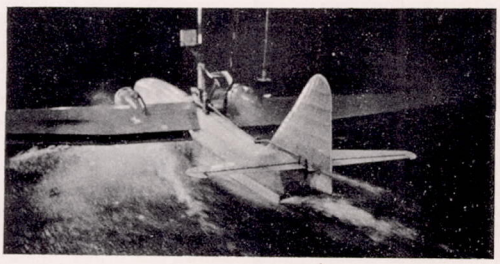

L/b, 15

V, 14.0 fps

V, 15.0 fps

NACA

(b) Gross load, 85 pounds.

Figure 14.- Continued.

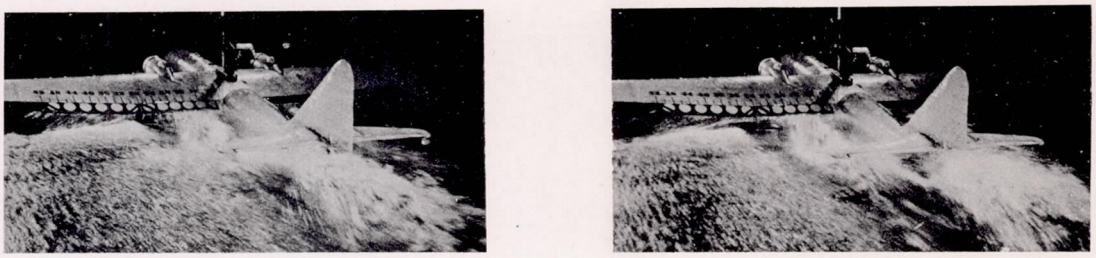

L/b, 9

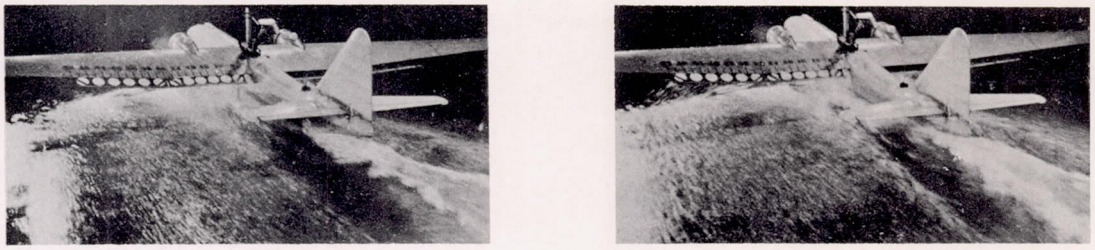

L/b, 12

V, 16.0 fps L/b, 15 V, 17.0 fps

(b) Continued.

Figure 14.- Continued.

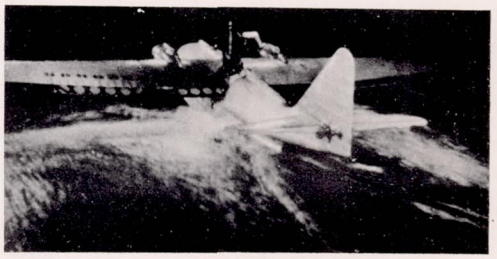

L/b, 6

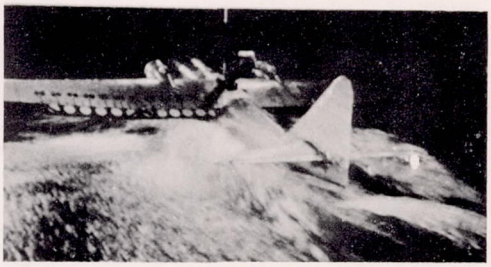

L/b, 9

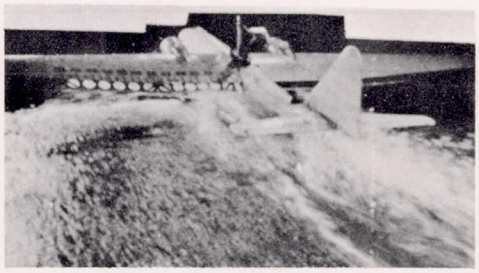

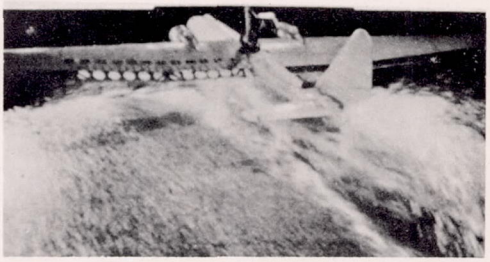

L/b, 12

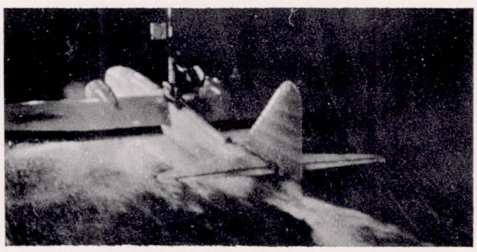

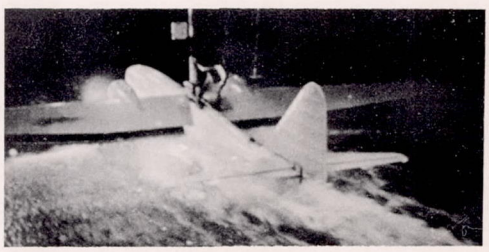

V, 18.0 fps

L/b, 15

V, 19.0 fps

NACA

(b) Concluded.

Figure 14.- Concluded.

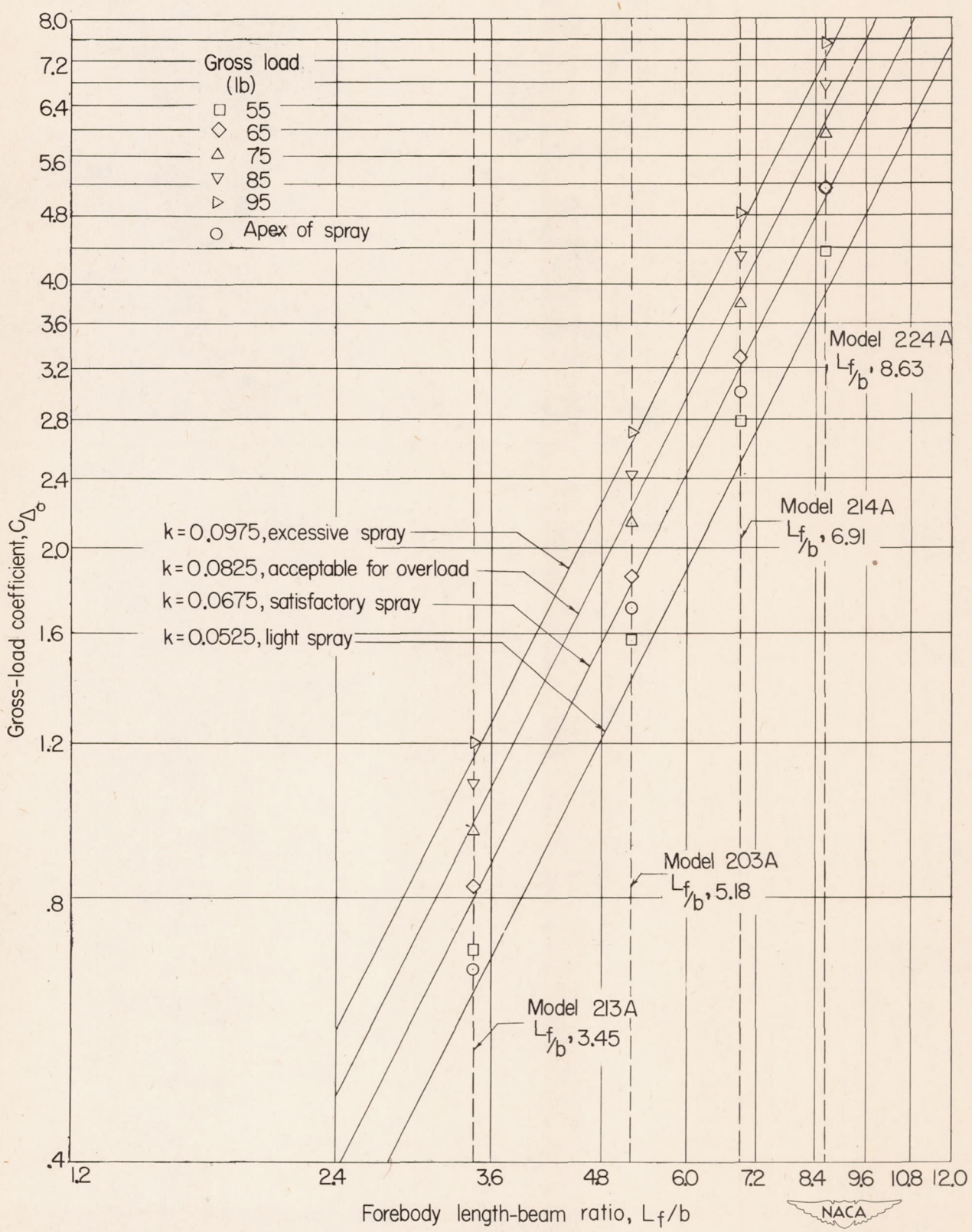

Figure 15.- Relationship between gross-load coefficient and forebody length-beam ratio.